TECHNICAL NOTE

D-180

HYDRODYNAMIC CHARACTERISTICS OF A PLANING SURFACE WITH CONVEX LONGITUDINAL CURVATURE AND AN ANGLE OF DEAD RISE OF 20°

By Elmo J. Mottard

Langley Research Center
Langley Field, Va.

NATIONAL AERONAUTICS AND SPACE ADMINISTRATION

WASHINGTON

January 1960

NATIONAL AERONAUTICS AND SPACE ADMINISTRATION

TECHNICAL NOTE D-180

HYDRODYNAMIC CHARACTERISTICS OF A PLANING SURFACE WITH CONVEX LONGITUDINAL CURVATURE AND AN ANGLE OF DEAD RISE OF 20°

By Elmo J. Mottard

SUMMARY

A hydrodynamic investigation was made in Langley tank no. 1 of a longitudinally curved planing surface with a dead-rise angle of 20°. The surface was a circular arc with the center of curvature 20 beams above the model. The beam was 4 inches and the length-beam ratio was 9. Wetted length, resistance, and trimming moment were determined for values of beam-load coefficient C_Δ from -3 to 37, Froude numbers from 6 to 25, and Reynolds numbers from 5×10^5 to 10^7.

Compared with a 0°-dead-rise surface with the same curvature, the 20°-dead-rise surface had a greater wetted-length—beam ratio (for the same lift), a lower lift-drag ratio, a more forward center-of-pressure location, and greater trim for maximum lift-drag ratio. Except at very low trim, the variation of the center-of-pressure location with wetted length was about the same for the 20°-dead-rise surface as for the 0°-dead-rise surface. The angle of the heavy-spray line at the wetted leading edge was the same as for a longitudinally straight surface with the same dead rise and leading-edge angle of incidence. The skin friction for the 20°-dead-rise curved surface was nearly the same as that for a plane surface alined parallel to the stream.

INTRODUCTION

Considerable data have been available for many years on the planing characteristics of longitudinally straight and concave planing surfaces. The data for straight surfaces are summarized in reference 1. Reference 2 contains data for concave surfaces. Until recently, however, although some planing craft have employed longitudinally convex surfaces, there has been no comparable supply of data for these surfaces.

In order to determine to what extent the planing characteristics would be affected by a slight longitudinal convexity, an experimental

investigation was undertaken at Langley tank no. 1 on convex surfaces having a radius of curvature of 20 beams and dead-rise angles of 0° and 20°. The results obtained with the 0°-dead-rise convex surface were reported in reference 3 and the results with the 20°-dead-rise convex surface are reported herein. The present results are compared with those of reference 3 and with the results from a longitudinally straight surface with 20° dead rise reported in reference 4.

SYMBOLS

b beam of planing surface, ft

$C_{D,b}$ drag coefficient based on square of beam, $\frac{R}{\frac{1}{2}\rho V^2 b^2}$

$C_{D,S}$ drag coefficient based on projected wetted area $l_{m,c}b$, $\frac{R}{\frac{1}{2}\rho V^2 l_{m,c}b}$ or $\frac{C_{D,b}}{l_{m,c}/b}$

$C_{f,a}$ skin-friction coefficient based on approximate mean velocity, $\frac{F_f}{\frac{1}{2}\rho V_{m,a}^2 l_m b \sec \beta}$

$C_{f,V}$ skin-friction coefficient based on forward speed, $\frac{F_f}{\frac{1}{2}\rho V^2 l_{m,c}b}$

$C_{L,b}$ lift coefficient based on square of beam, $\frac{F_V}{\frac{1}{2}\rho V^2 b^2}$ or $\frac{2C_\Delta}{C_V^2}$

$C_{L,S}$ lift coefficient based on projected wetted area $l_{m,c}b$, $\frac{F_V}{\frac{1}{2}\rho V^2 l_{m,c}b}$ or $\frac{C_{L,b}}{l_{m,c}/b}$

C_R resistance coefficient, R/wb^3

C_V speed coefficient or Froude number, $V/\sqrt{gb}$

C_Δ load coefficient or beam loading, F_V/wb^3

d draft of trailing edge at keel referred to undisturbed water surface, ft

d_c draft of trailing edge of chord of mean wetted arc at keel referred to undisturbed water surface, ft

F_f friction force tangential to planing surface, M_f/r, lb

F_v vertical force (lift, positive upwards), lb

g acceleration due to gravity, 32.2 ft/sec^2

l_c length of arc between trailing edge and heavy spray line at chine, ft

l_k length of arc between trailing edge and heavy spray line at keel, ft

l'_m length of arc between trailing edge and rear mean boundary of wetted area, ft

l_m length of arc between front and rear mean boundaries of wetted area, ft

$l_{m,c}$ length of chord between front and rear mean boundaries of wetted area, ft

$l_{p,c}$ distance along mean chord at keel from rear mean boundary of wetted area to intersection with resultant force vector,

$$\frac{1}{2}l_{m,c} + \sqrt{r^2 - \left(\frac{l_{m,c}}{2}\right)^2}\,\tan\left(\tan^{-1}\frac{R}{F_v} - \tau_c\right)$$

$$+ \frac{M_k}{F_v}\cos\left(\tan^{-1}\frac{R}{F_v}\right)\sec\left(\tan^{-1}\frac{R}{F_v} - \tau_c\right)$$

M_k trimming moment about center of curvature of keel, lb-ft

M_f trimming moment about center of curvature of bottom midway between keel and chine, lb-ft

r radius of curvature of planing-surface bottom, ft

R horizontal force (drag, positive rearward), lb

$N_{Re,a}$ Reynolds number based on approximate mean velocity, $\frac{V_{m,a} l_m}{\nu}$

V speed, fps

$V_{m,a}$ approximate mean velocity over planing surface, $\sqrt{V^2\left(1 - \frac{C_{L,b}}{\frac{l_{m,c}}{b} \cos \tau_c}\right)}$, fps

w specific weight of water, lb/cu ft

β angle of dead rise (measured in planes perpendicular to base line; see fig. 1), deg

ρ mass density of water, slug/cu ft

τ trim (angle between base line and horizontal; see fig. 1), deg

τ_c trim of mean chord (angle between chord of mean wetted arc and horizontal), deg

τ_l trim of tangent to planing surface at front mean boundary, $\tau + \frac{90}{\pi r}\left(l_c + l_k\right)$, deg

ν kinematic viscosity, ft^2/sec

DESCRIPTION OF MODEL

The model, shown in figure 1, had a longitudinally curved bottom with the center of the curvature located 80 inches above the model. The angle of dead rise (defined as the angle measured in planes perpendicular to the tangent at the trailing edge) was 20°. The beam was 4 inches and the length 36 inches. The mean radius of curvature of the chines was less than 0.002 inch. The model was constructed of steel with a plastic bottom covering. The bottom was white with black lines every inch along the arc to facilitate reading wetted lengths.

APPARATUS AND PROCEDURE

Tests

The tests were conducted in Langley tank no. 1 which, together with the apparatus for towing the model and the instrumentation for measuring the lift, drag, and trimming moment about the center of curvature of the model, has been described in reference 5. A schematic representation of the model and towing gear is presented in figure 2. Wetted length, resistance, and trimming moment were determined for values of beam-load coefficient C_{Δ} from -3 to 37, Froude numbers from 6 to 25, and Reynolds numbers from 5×10^5 to 10^7.

The test procedures were similar to those described in reference 6. The trim, load, and speed were held constant during each test run. The trim and draft were measured at the trailing edge of the model. The wetted lengths were obtained from underwater photographs of the bottom. A typical photograph is presented in figure 3.

Data Analysis

The method of data analysis which was used in reference 3 and is again used here is briefly explained with the aid of figure 4, in which the represented quantities are scaled from the data for the test run depicted in figure 3(c). Front and rear "mean boundaries" were selected to facilitate representation of wetted areas and wetted chord lengths. The mean boundary was defined as a transverse line located midway between the intersections of the wetted area with the keel and chine. These mean boundaries define a rectangular region equal in area to the actual wetted area. The wetted length l_m is then defined as the length of this region. The locations of the front and rear mean boundaries were determined from measurements on photographs of the bottom, such as figure 3.

The "mean chord at the keel" was defined as a longitudinal straight line between the front and rear mean boundaries at the keel. The length of the mean chord $l_{m,c}$ was computed from the locations of the front and rear mean boundaries. The maximum difference between the arc wetted length l_m and the chord wetted length $l_{m,c}$ was less than 0.33 percent.

The trim of the mean chord τ_c was computed from the trailing-edge trim τ and the locations of the front and rear mean boundaries. The draft d_c of the keel at the trailing edge of the mean wetted area was computed from the draft d of the model trailing edge at the keel, the trailing-edge trim τ, and the location l'_m of the rear mean boundary.

As in references 3 and 7, buoyant effects have not been subtracted out of the data, but large buoyant effects have been excluded by including only test runs with buoyant force less than 20 percent of the total lift.

Because of the circular-arc curvature of the model, only tangential forces can cause a moment about the center of curvature. It is therefore possible to obtain resultant friction force by dividing the moment about the center of curvature by the radius of curvature. However, because the center of curvature varies from the keel to the chine (see fig. 1), the moment M_f about a center midway between these two centers was used. The resulting error in the friction force is less than 0.45 percent. In the absence of pressure data the mean velocity, and therefore also the friction coefficient and Reynolds number, were approximated. In the calculation of the approximate mean velocity, the mean pressure on the planing surface was assumed equal to $\frac{\text{Total lift}}{\text{Horizontal projection of wetted area}}$.

RESULTS AND DISCUSSION

The data are presented in the conventional nondimensional form in table I and in figures 5 to 9. In figures 9 to 14 comparisons are made with the 0°-dead-rise convex surface of reference 3 and the 20°-dead-rise straight surface of reference 4. The effects of convexity are discussed in more detail in reference 3.

The effect of longitudinal convexity on the flow pattern may be deduced with the aid of figure 3. The flow for the curved surface shown by the underwater photograph in figure 3(a) is similar to the flow on a longitudinally straight planing surface for trailing-edge trim settings of 5.75° or greater. In this flow pattern the rear portion of the bottom is always entirely wetted. For the curved surface at lower trim settings, the principal wetted area at the rear tapers toward the center line (fig. 3(b)). The length of the tapered area increases as the trim is decreased (a decrease in trim may be regarded as an extension rearward of the model along its arc). At the trim settings of -5.75° and -8.75°, the trailing edge of the model is behind the principal wetted area, which converges to a point, as shown in figure 3(c). This convergence of the wetted area is independent of dead rise and occurs because the flow, in following the model, requires vertical divergence at the rear. The vertical divergence occurs near a free (constant-pressure) surface which prevents appreciable slowing down in the flow. It is therefore accompanied by a horizontal convergence, which is apparent in figure 3(c).

The lift, wetted length, center-of-pressure location, drag, draft, and length of the triangular portion at the front of the wetted area are presented in nondimensional form in figures 5 to 9. When plotted against the lift coefficient $C_{L,b}$, the nondimensional wetted length $l_{m,c}/b$ (fig. 5), center-of-pressure location $l_{p,c}/b$ (fig. 6), drag coefficient $C_{D,b}$ (fig. 7), and draft d_c/b (fig. 8) each fall along a single line for each trim. Negative lift was obtained at trims of -5.75° and -8.75° but was limited to lift coefficients of -0.02. At trailing-edge trims more negative than -5.75°, the data are the same as at -5.75° because the flow is not influenced by the trailing-edge trim. At trailing-edge trims more negative than -5.75° and values of $C_{L,b}$ near zero, the location of the center of pressure $l_{p,c}$ (fig. 6) varies greatly with $C_{L,b}$ and evidently approaches positive or negative infinity as the resultant force vector becomes parallel with the mean chord line from the direction of positive or negative lift. This type of result does not exist for a prismatic surface but may be obtained on a convex surface because of the existence of both positive and negative pressures, as discussed in reference 3. The length $\frac{l_k - l_c}{b}$ of the triangular portion at the front of the wetted area is plotted against the mean trim τ_l of this triangular portion in figure 9. The results fall along a single line and are in good agreement with theoretical and experimental results from planing surfaces without curvature presented in reference 4.

In figure 10 the nondimensional length $l_{m,c}/b$ of the line between the front and rear mean boundaries is plotted against $C_{L,b}$ for various values of the trim of this line. The dashed lines are results with zero dead rise from reference 3. The percent reduction in lift due to 20° dead rise was greatest at low trim and varied from about 18 percent at 30° to 60 percent at 4°. Although there were some negative values of $C_{L,b}$ (fig. 5), they do not appear in figure 10 because there were insufficient data to obtain cross plots in this region.

In figures 10 and 11 the upper ends of the curves for $\tau_c = 4^\circ$ and 6° define the maximum wetted lengths obtainable. An increase in wetted length l_m at constant τ results in an increase in τ_c so that the curves of τ_c = Constant may be traversed only by regarding each increase in wetted length as accompanied by a compensating decrease in τ. At small values of τ_c a point is reached where the trailing edge is not wetted (as in fig. 3(b)), and decreasing τ no longer compensates for increasing l_m.

The location of the center of pressure $l_{p,c}/b$ is plotted against $C_{L,b}$ in figure 11. The curves appear similar to those of figure 10 in

that, for a given value of lift coefficient, an increase in $l_{m,c}/b$ was accompanied by a corresponding increase in $l_{p,c}/b$.

The center-of-pressure location $l_{p,c}/b$ is plotted against $l_{m,c}/b$ in figure 12 for the 20°-dead-rise surface and the 0°-dead-rise surface of reference 3. Dead rise had very little effect on $l_{p,c}$ at values of trim τ_c above 4°. At 4° trim the center of pressure was located a maximum distance of 1 beam further forward on the 20°-dead-rise model.

In figure 13 the nondimensional draft d_c/b referred to the undisturbed water surface is plotted against the nondimensional draft $\frac{l_{m,c}}{b} \sin \tau_c$ referred to the water surface at the wetted leading edge. At high trim the draft referred to the water surface at the wetted leading edge was greater (the points lie below the dashed 45° line); thus, pile-up is indicated. The results presented here are similar to those for the 0°-dead-rise surface in reference 3, except that the 0°-deadrise surface gave slightly larger pile-up at high trim.

The lift-drag ratios for the 20°- and 0°-dead-rise convex surfaces are compared in figure 14. The 20°-dead-rise surface had a slightly smaller lift-drag ratio and larger trim for maximum lift-drag ratio.

The skin-friction coefficient and Reynolds number as defined in the section on data analysis are plotted in figure 15. The data in figure 15 show no correlation with trim. The scatter is great at high trim because the friction force is small relative to the lift and drag forces from which it was obtained, and the accuracy is therefore poor. Comparison of the data points with a typical transition curve for a flat plate (ref. 8) shows what may be considered fair agreement for data in the transition range. The slight delay in transition is probably due to the favorable pressure gradient.

CONCLUSIONS

An analysis of experimental data obtained in an investigation of a 20°-dead-rise longitudinally convex planing surface leads to the following conclusions:

1. The effects of increasing the dead rise of a convex surface from 0° to 20° are (for a given lift) to increase the wetted length-beam ratio, decrease the lift-drag ratio, and increase the trim for maximum lift-drag ratio. These effects are the same as have been found for a longitudinally straight surface. The variation of the center-of-pressure location with wetted length was about the same for the 20°-dead-rise surface as for the 0°-dead-rise surface for trims above 4°.

At 4° trim the center of pressure was further forward on the 20°-dead-rise surface.

2. The angle of the heavy spray line at the leading edge was about the same as for a longitudinally straight surface with the same dead rise and leading-edge angle of incidence.

3. The skin friction for the 20°-dead-rise curved surface was nearly the same as for a plane surface alined parallel to the stream.

Langley Research Center,
National Aeronautics and Space Administration,
Langley Field, Va., September 1, 1959.

REFERENCES

1. Shuford, Charles L., Jr.: A Theoretical and Experimental Study of Planing Surfaces Including Effects of Cross Section and Plan Form. NACA Rep. 1355, 1958. (Supersedes NACA TN 3939.)

2. Sottorf, W.: Experiments With Planing Surfaces. NACA TM 739, 1934.

3. Mottard, Elmo J.: Effect of Convex Longitudinal Curvature on the Planing Characteristics of a Surface Without Dead Rise. NASA MEMO 1-25-59L, 1959.

4. Chambliss, Derrill B., and Boyd, George M., Jr.: The Planing Characteristics of Two V-Shaped Prismatic Surfaces Having Angles of Dead Rise of 20° and 40°. NACA TN 2876, 1953.

5. Truscott, Starr: The Enlarged N.A.C.A. Tank, and Some of Its Work. NACA TM 918, 1939.

6. Kapryan, Walter J., and Weinstein, Irving: The Planing Characteristics of a Surface Having a Basic Angle of Dead Rise of 20° and Horizontal Chine Flare. NACA TN 2804, 1952.

7. Weinstein, Irving, and Kapryan, Walter J.: The High-Speed Planing Characteristics of a Rectangular Flat Plate Over a Wide Range of Trim and Wetted Length. NACA TN 2981, 1953.

8. Davidson, Kenneth S. M.: Resistance and Powering. Detailed Considerations - Skin Friction. Vol. II of Principles of Naval Architecture, ch. II, pt. 2, sec. 7, Henry E. Rossell and Lawrence B. Chapman, eds., Soc. Naval Arch. and Marine Eng., 1939, pp. 76-83.

TABLE I.- EXPERIMENTAL DATA FOR A LONGITUDINALLY CONVEX PLANING SURFACE HAVING A RADIUS OF CURVATURE 20 TIMES THE BEAM AND AN ANGLE OF DEAD RISE OF 20°

[Average kinematic viscosity, 12.04 × 10^{-6} ft^2/sec; specific weight of tank water, 63.4 lb/cu ft]

C_Δ	C_V	C_R	$\frac{l_c}{b}$	$\frac{l_k}{b}$	$\frac{l_m}{b}$	$\frac{l_{m,c}}{b}$	$\frac{d_c}{b}$	$C_{L,b}$	$C_{D,b}$	$C_{L,s}$	$C_{D,s}$	$C_{f,V}$	$\frac{l_{p,c}}{b}$
τ = 11.75°													
6.51	6.17	2.21	2.39	2.69	0	2.54	----	0.3416	0.1160	0.1346	0.0457	0.0032	1.84
8.68	9.27	2.47	1.18	1.53	0	1.36	----	.2022	.0576	.1485	.0423	.0022	1.15
15.20	12.34	4.08	1.11	1.48	0	1.30	0.29	.1996	.0536	.1538	.0412	.0012	1.00
23.87	9.37	9.54	3.97	4.20	0	4.07	1.15	.5440	.2172	.1336	.0534	.0032	3.06
23.88	12.43	7.55	2.14	2.44	0	2.29	.55	.3090	.0978	.1725	.0546	.0032	1.94
28.22	15.60	8.06	1.43	1.79	0	1.61	----	.2316	.0662	.1454	.0411	.0019	1.23
32.55	12.46	11.61	2.99	3.24	0	3.12	.83	.4190	.1496	.1343	.0480	.0028	2.37
36.90	12.53	13.69	3.34	3.59	0	3.47	.94	.4700	.1744	.1355	.0503	.0021	2.74
τ = 17.75°													
13.02	6.20	6.14	3.29	3.47	0	3.38	1.14	0.6782	0.3198	0.2007	0.0946	0.0022	2.43
13.02	12.43	4.54	.40	.70	0	.55	.16	.1684	.0588	.3062	.1069	.0010	.46
19.53	9.27	8.21	2.06	2.29	0	2.18	.66	.4344	.1826	.1992	.0838	.0027	1.51
19.53	13.97	6.97	.60	.88	0	.74	.21	.2000	.0714	.2702	.0965	.0022	.51
23.87	12.37	9.08	1.23	1.48	0	1.36	.38	.3120	.1186	.2294	.0872	.0017	.94
32.55	10.87	14.29	2.67	2.87	0	2.77	.91	.5508	.2418	.1988	.0873	.0016	1.98
32.55	15.53	11.96	.96	1.23	0	1.10	.34	.2700	.0992	.2455	.0902	.0012	.76
36.89	15.60	13.73	1.18	1.46	0	1.32	.55	.3032	.1128	.2297	.0855	.0024	.74
τ = 23.75°													
8.68	6.32	4.40	1.43	1.61	0	1.52	0.56	0.4350	0.2204	0.2862	0.1450	0.0015	1.02
8.68	7.74	4.26	.80	1.03	0	.92	.39	.2898	.1422	.3150	.1545	.0029	.67
23.87	14.06	11.20	.58	.78	0	.68	.32	.2414	.1132	.3550	.1664	.0008	.45
32.55	10.81	17.13	1.89	2.06	0	1.98	.72	.5568	.2930	.2812	.1479	.0012	1.53
36.89	15.53	17.54	.70	1.01	0	.90	.30	.3058	.1450	.3398	.1611	-.0006	.59
τ = 29.75°													
8.68	6.29	5.41	1.16	1.28	0	1.22	0.53	0.4384	0.2732	0.3593	0.2239	0.0012	0.71
15.19	7.74	9.66	1.38	1.51	0	1.44	.65	.5072	.3226	.3522	.2240	.0002	.89
32.55	13.88	19.95	.78	.91	0	.84	.38	.3378	.2070	.4021	.2464	.0002	.59
τ = -0.25°													
4.34	9.21	1.51	4.07	4.60	0.13	4.20	0.50	0.1012	0.0356	0.0241	0.0085	0.0024	4.82
4.34	12.28	1.71	3.22	3.87	.08	3.46	.36	.0576	.0226	.0166	.0065	.0026	4.63
6.51	21.92	3.60	2.52	3.37	.06	2.88	.28	.0270	.0150	.0094	.0052	.0030	4.58
10.85	18.85	4.39	3.29	3.97	.13	3.50	.38	.0610	.0248	.0174	.0071	.0030	4.52
13.02	25.05	5.87	2.62	3.37	.05	2.95	.32	.0414	.0188	.0140	.0064	.0031	4.54
21.70	15.75	7.42	4.93	5.36	.30	4.84	.70	.1750	.0598	.0361	.0124	.0029	4.86
28.21	18.85	10.08	4.90	5.36	.28	4.84	.67	.1488	.0568	.0307	.0117	.0028	5.10
32.55	15.69	12.05	6.04	6.39	.38	5.81	.97	.2644	.0978	.0455	.0168	.0026	5.73
34.72	12.49	14.43	7.55	7.87	.38	7.31	1.18	.4452	.1850	.0609	.0253	.0030	6.66
τ = 5.75°													
4.34	9.24	0.83	1.13	1.79	----	1.46	0.19	0.1016	0.0184	0.0696	0.0126	0.0017	1.29
10.85	9.30	3.24	3.42	3.82	----	3.62	.71	.2508	.0750	.0693	.0207	.0026	3.09
15.19	12.53	3.98	2.77	3.22	----	3.00	.55	.1936	.0508	.0645	.0169	.0020	2.53
15.19	15.60	3.44	1.66	2.24	----	1.92	.34	.1248	.0282	.0650	.0147	.0025	1.72
19.53	9.24	7.40	5.26	5.53	----	5.39	1.23	.4574	.1734	.0849	.0322	.0031	4.58
19.53	9.30	7.44	5.23	5.53	----	5.37	1.23	.4516	.1720	.0841	.0320	.0023	4.55
23.87	9.27	9.63	5.96	6.21	----	6.06	1.47	.5558	.2242	.0917	.0370	.0034	4.98
23.87	12.31	7.63	4.12	4.45	----	4.27	.81	.3152	.1006	.0738	.0236	.0020	3.52
28.21	12.37	9.65	4.60	4.90	----	4.74	.95	.3688	.1262	.0778	.0266	.0021	4.08
28.21	18.42	7.08	2.29	2.79	----	2.54	.38	.1662	.0418	.0654	.0165	.0025	2.19
τ = -8.75°													
-3.25	18.60	2.35	4.53	5.61	1.61	3.46	----	0.0188	0.0136	-0.0054	0.0039	0.0030	-1.28
2.17	15.41	2.26	5.53	6.39	1.81	4.14	----	.0182	.0190	.0044	.0046	.0026	8.70
6.51	18.60	3.95	5.94	6.64	2.00	4.28	----	.0276	.0228	.0064	.0053	.0026	6.60
13.00	21.70	6.49	6.28	6.94	2.12	4.48	----	.0550	.0274	.0123	.0061	.0027	6.26
21.70	18.48	8.40	7.47	7.94	2.46	5.24	----	.1262	.0488	.0241	.0093	.0029	5.76
23.90	24.80	10.16	6.72	7.27	2.25	4.74	----	.0778	.0330	.0164	.0049	.0028	5.73
τ = -5.75°													
-1.09	15.35	1.67	3.75	4.75	0.74	3.51	0.15	-0.0093	0.0142	-0.0026	0.0040	0.0033	-4.85
1.09	9.27	.83	4.78	5.51	.70	4.44	.27	.0254	.0194	.0057	.0044	.0022	8.51
2.17	9.24	1.10	5.26	5.94	.88	4.71	.35	.0508	.0258	.0108	.0055	.0018	7.45
4.34	7.68	1.61	6.72	7.17	1.00	5.93	----	.1472	.0546	.0248	.0092	.0020	6.68
10.85	15.44	4.45	5.78	6.36	1.33	4.73	.47	.0846	.0374	.0179	.0058	.0028	5.75
10.85	18.57	5.08	5.31	5.99	1.28	4.36	.39	.0630	.0294	.0144	.0067	.0029	5.83
10.85	21.61	5.80	5.13	5.76	1.22	4.22	----	.0464	.0248	.0110	.0059	.0028	6.14
10.85	24.77	7.02	4.88	5.55	1.11	4.10	----	.0254	.0228	.0064	.0057	.0030	7.43
14.11	12.31	5.36	7.12	7.57	1.48	5.85	.77	.1862	.0708	.0318	.0121	.0027	6.22
17.36	12.31	6.45	7.65	8.02	1.50	6.32	.87	.2292	.0852	.0363	.0135	.0021	6.54
23.87	18.57	9.19	6.51	7.02	1.48	5.28	.61	.1584	.0534	.0262	.0101	.0030	5.76

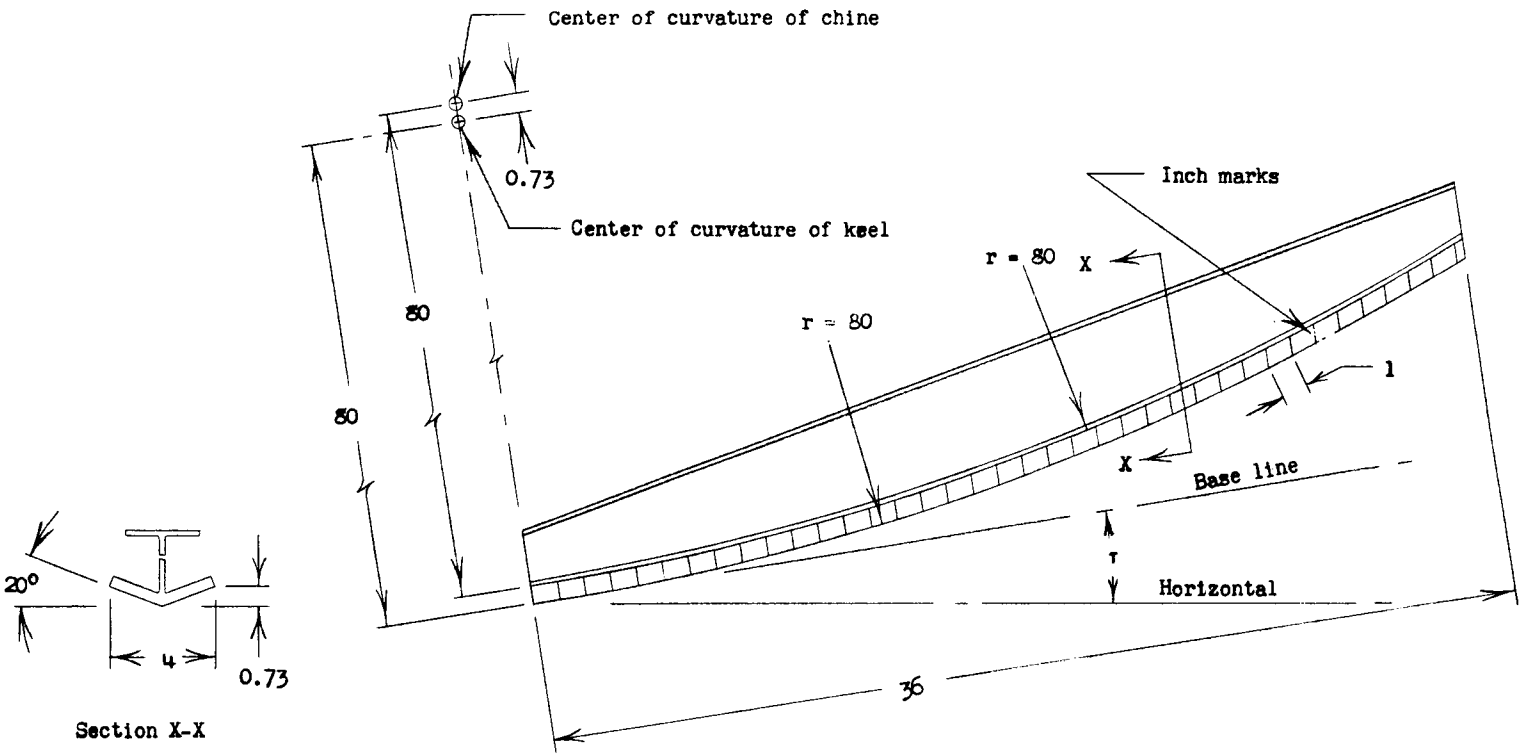

Figure 1.- Sketch of model. Dimensions are in inches.

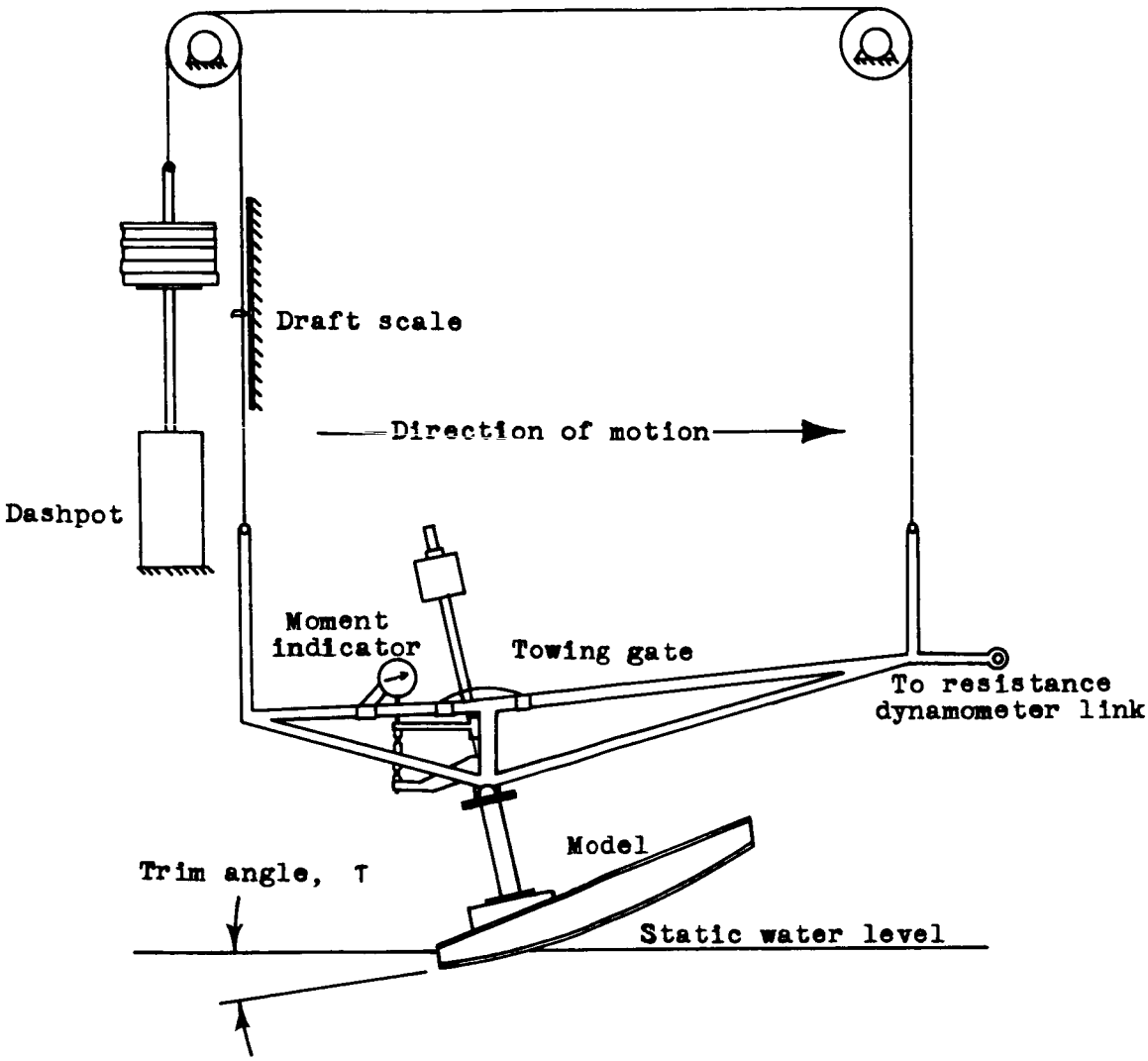

Figure 2.- Model on towing gear.

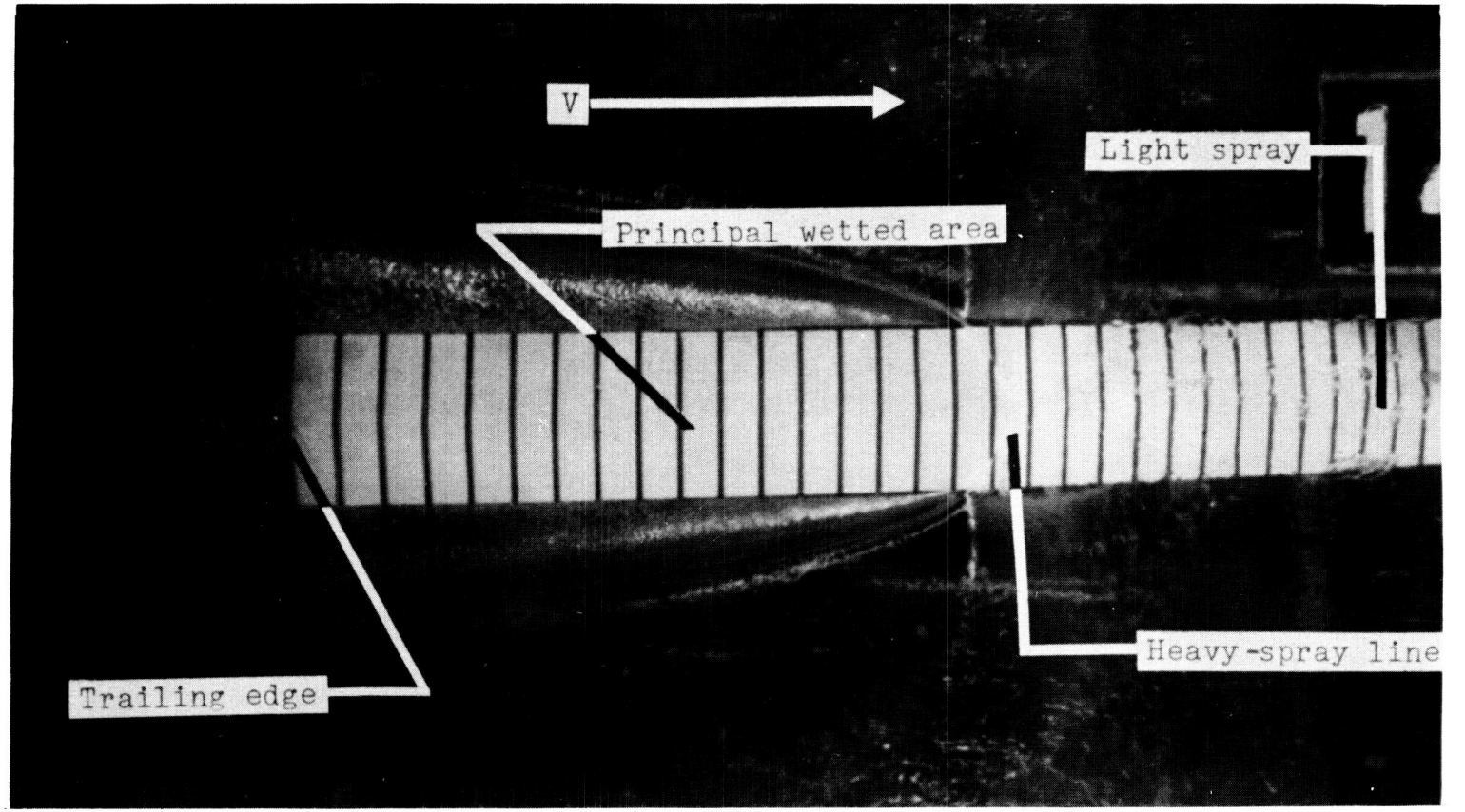

(a) $\tau = 5.75^{\circ}$.

L-59-6067

Figure 3.- Typical underwater photographs.

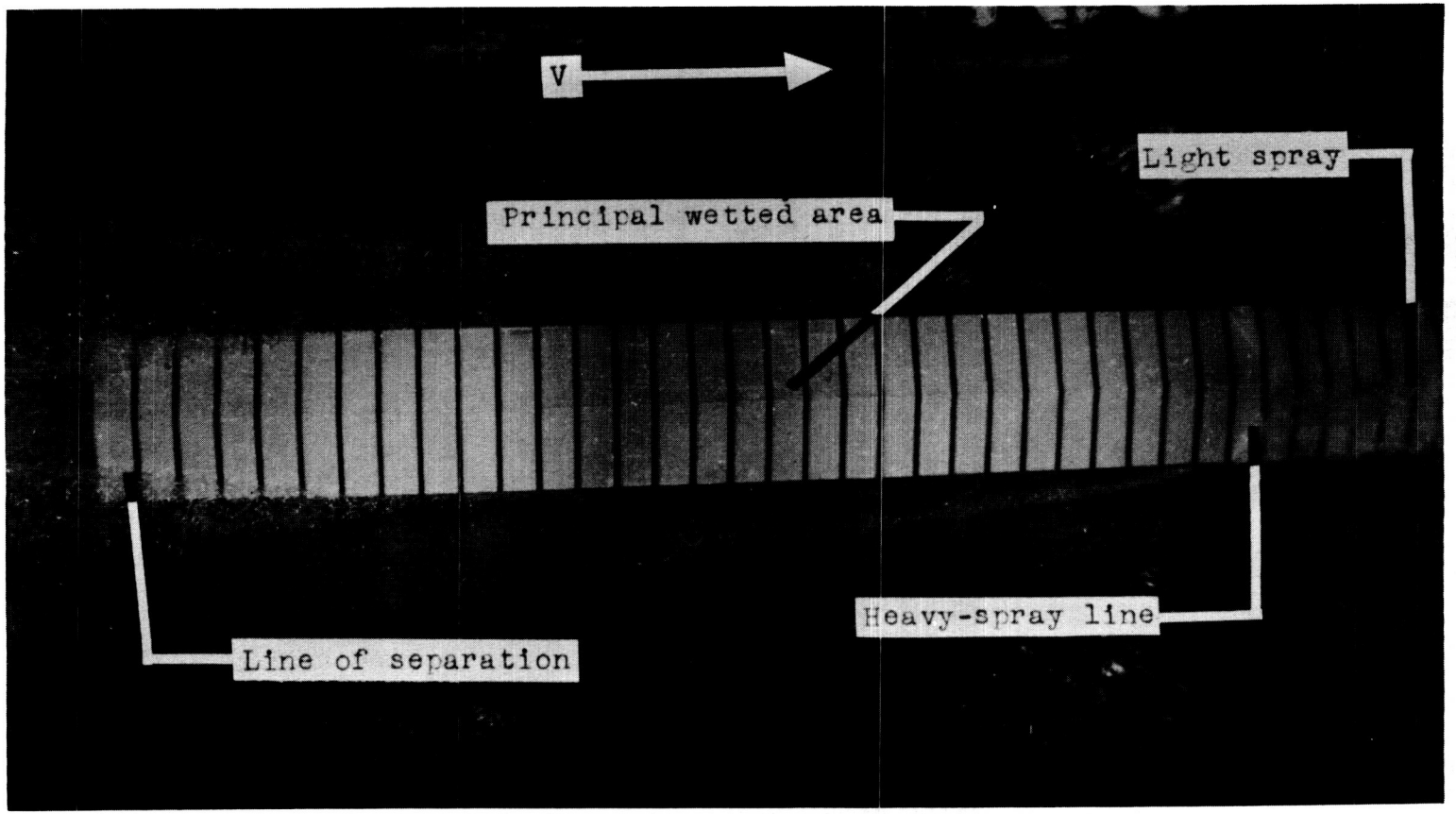

(b) $\tau = -0.25^{\circ}$. L-59-6068

Figure 3.- Continued.

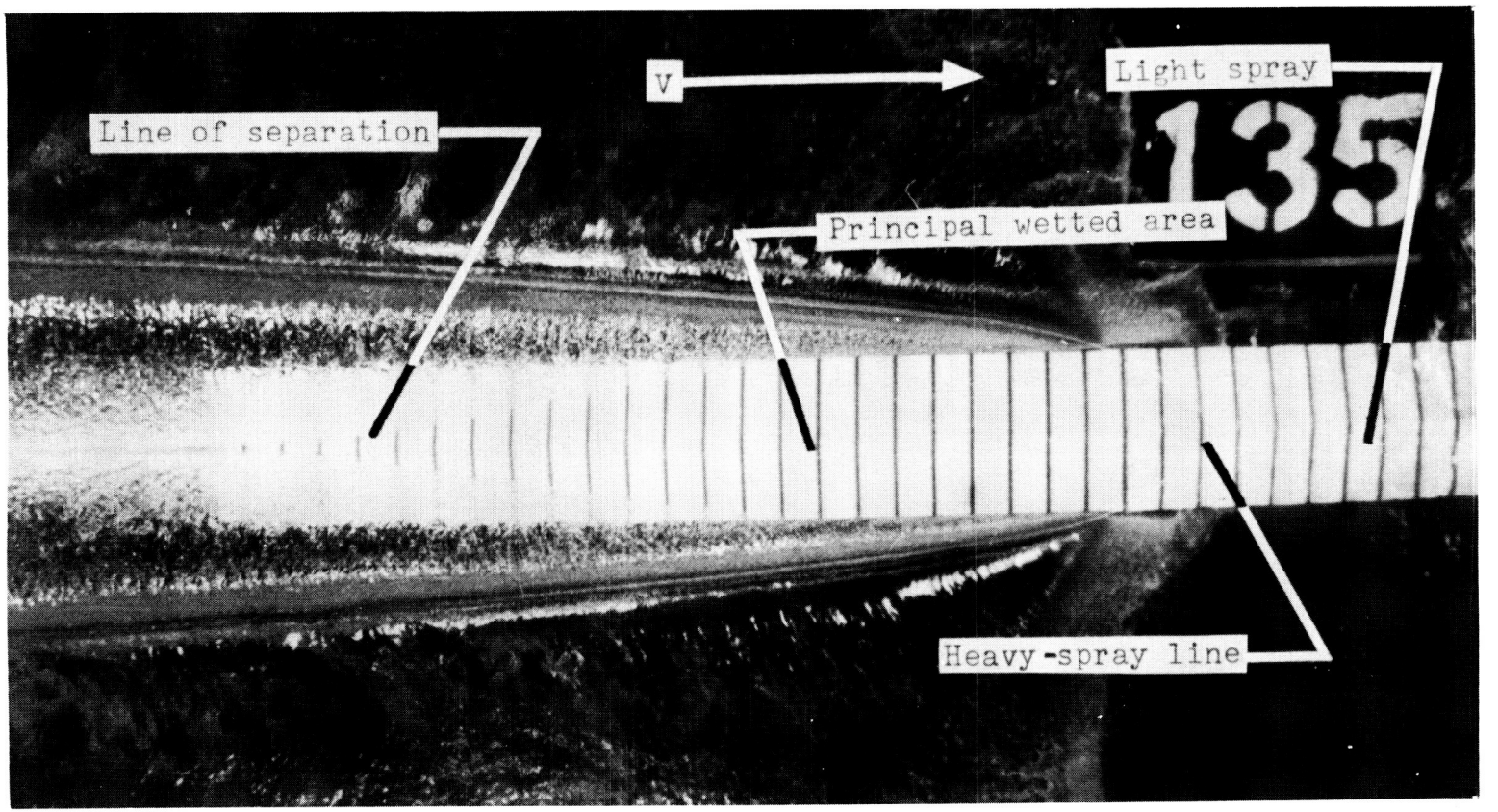

(c) $\tau = -8.75^{\circ}$. L-59-6069

Figure 3.- Concluded.

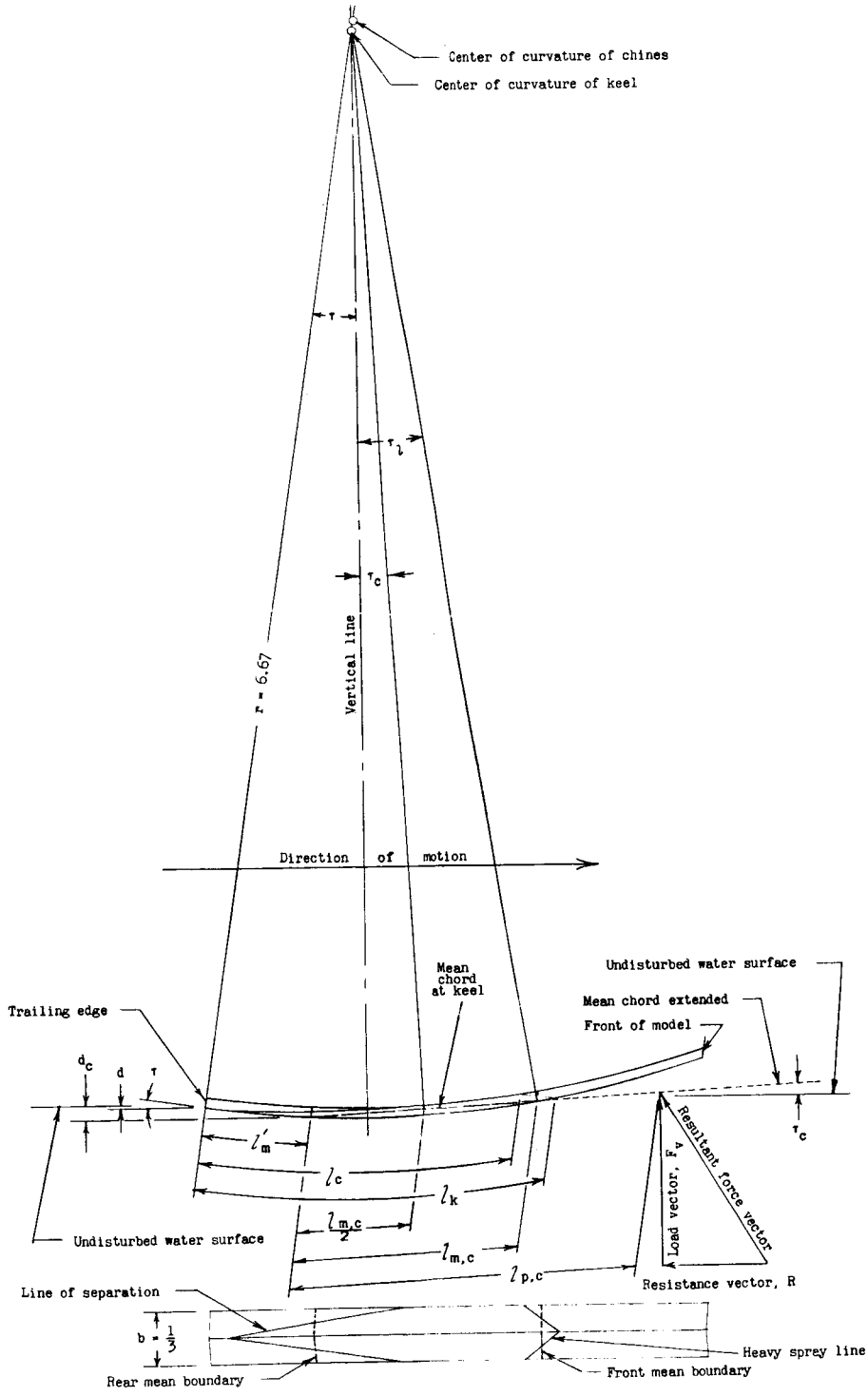

Figure 4.- Sketch of model during test run. Dimensions are in feet.

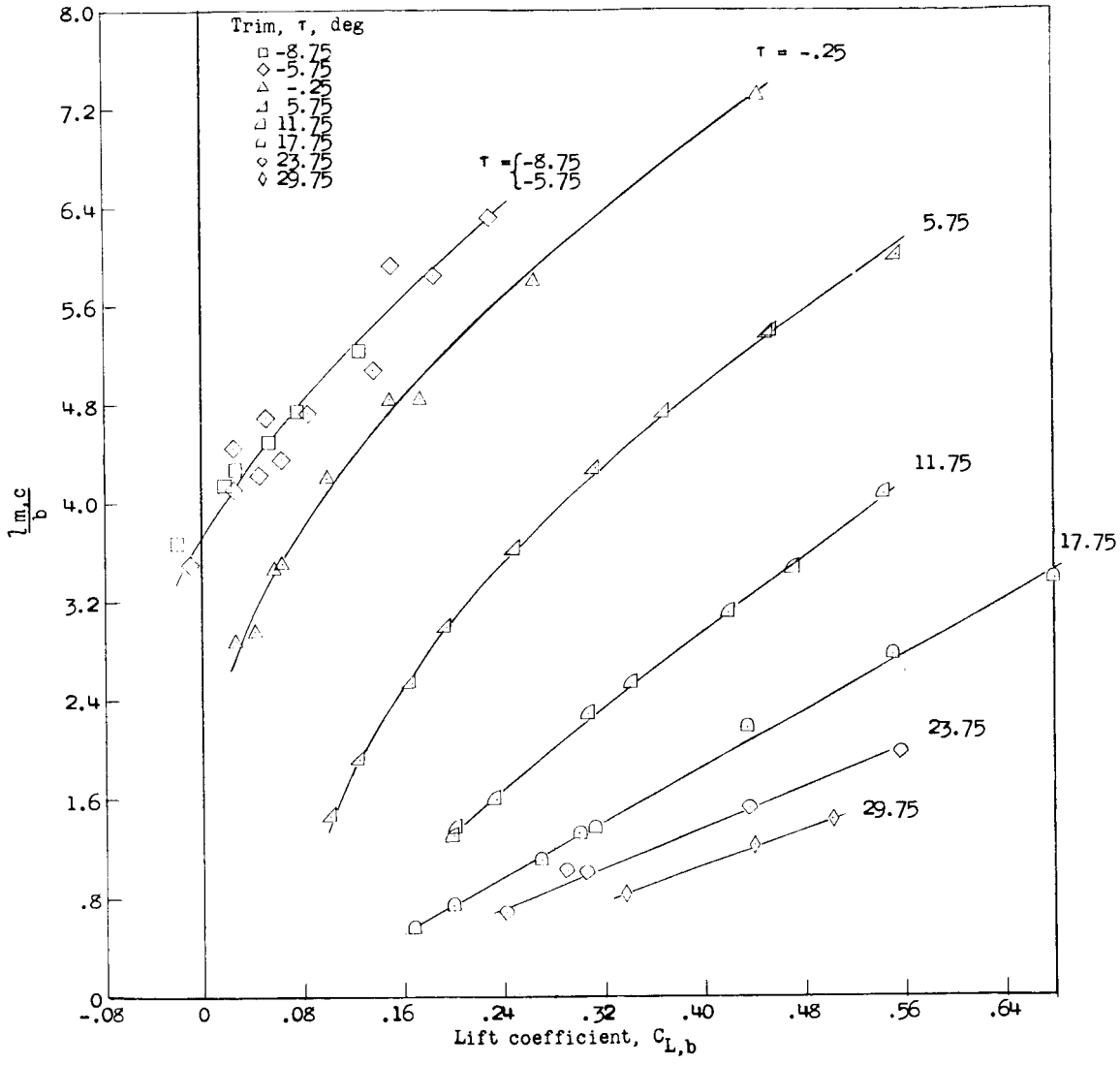

Figure 5.- Variation of mean wetted-length—beam ratio with lift coefficient for several values of trim at the trailing edge.

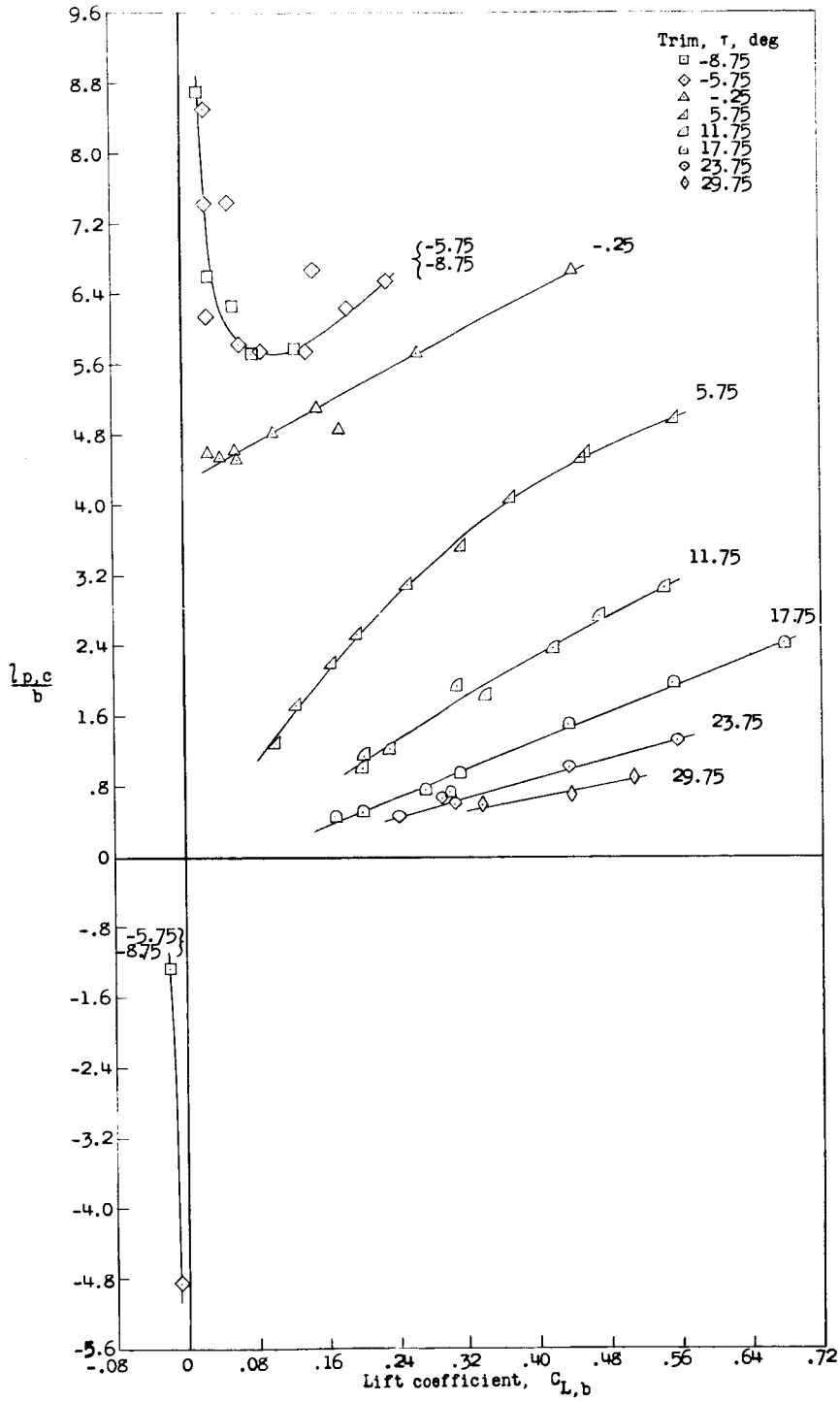

Figure 6.- Variation of center-of-pressure location with lift coefficient.

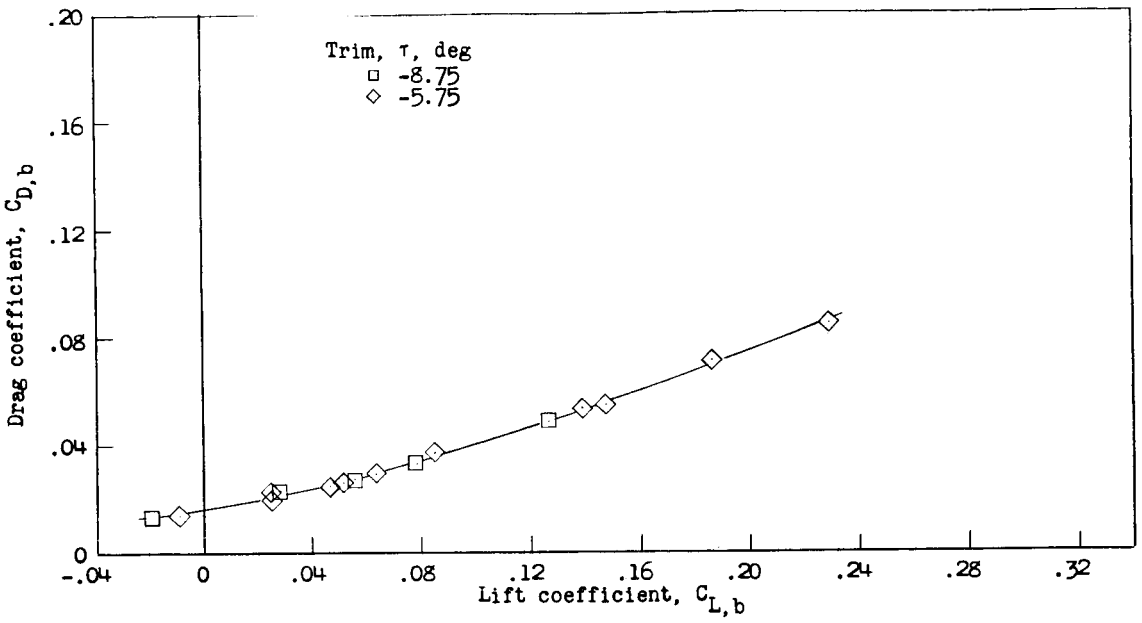

(a) Trim: -8.75° and -5.75°.

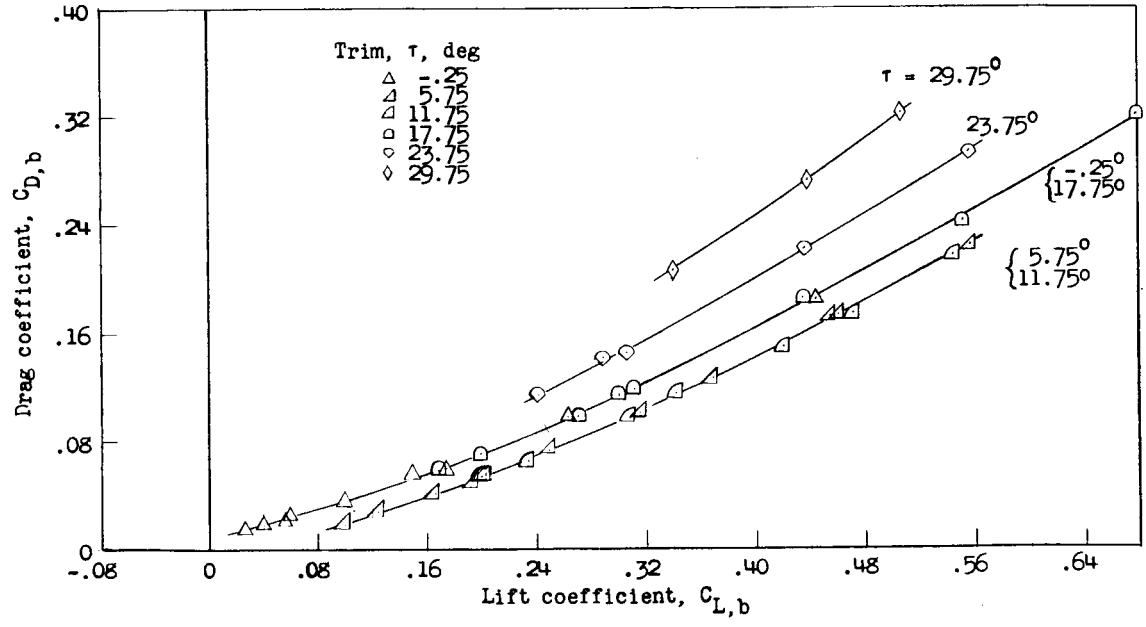

(b) Trim: -0.25°, 5.75°, 11.75°, 17.75°, 23.75°, and 29.75°.

Figure 7.- Variation of drag coefficient with lift coefficient for several values of trim at the trailing edge.

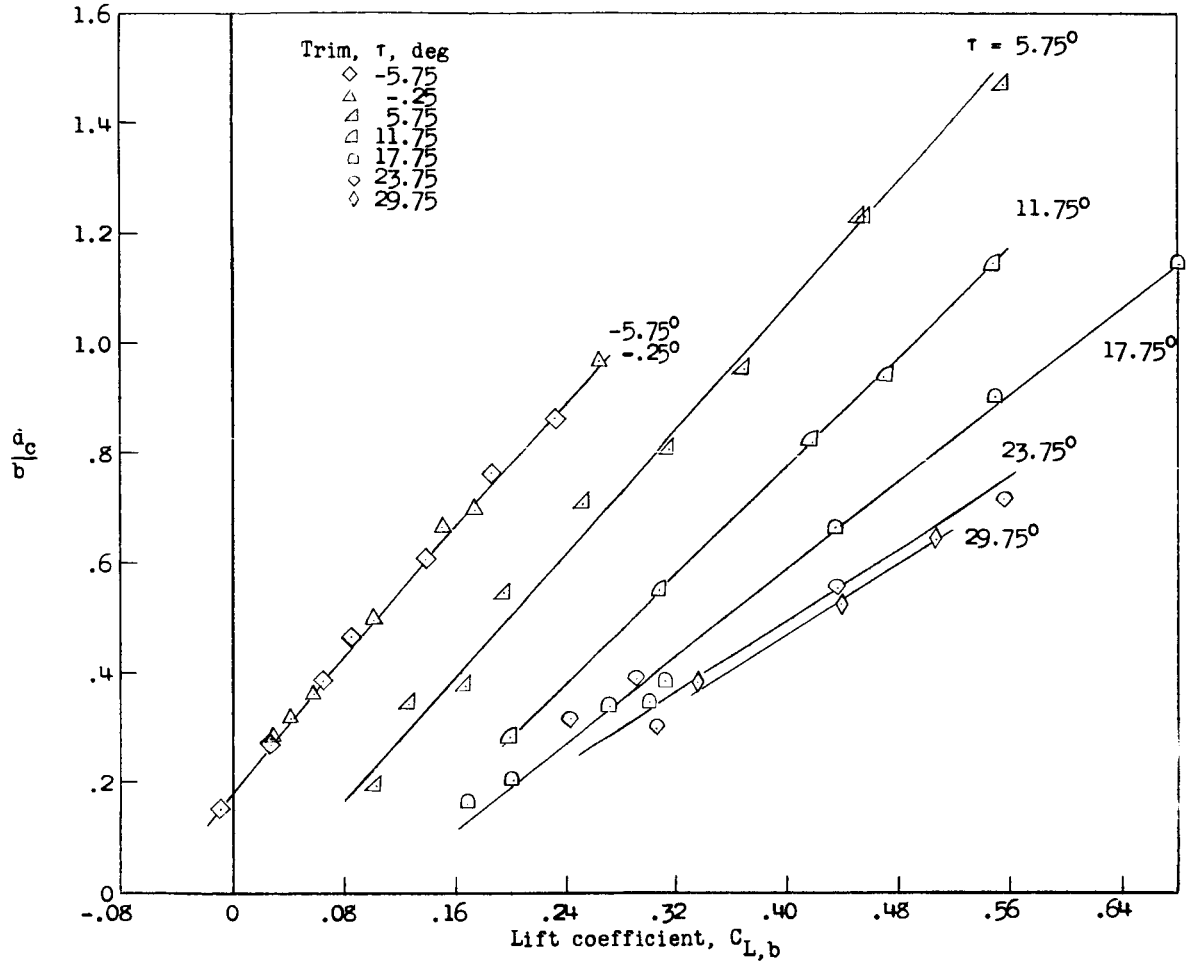

Figure 8.- Variation of nondimensional draft with lift coefficient for several values of trim at the trailing edge.

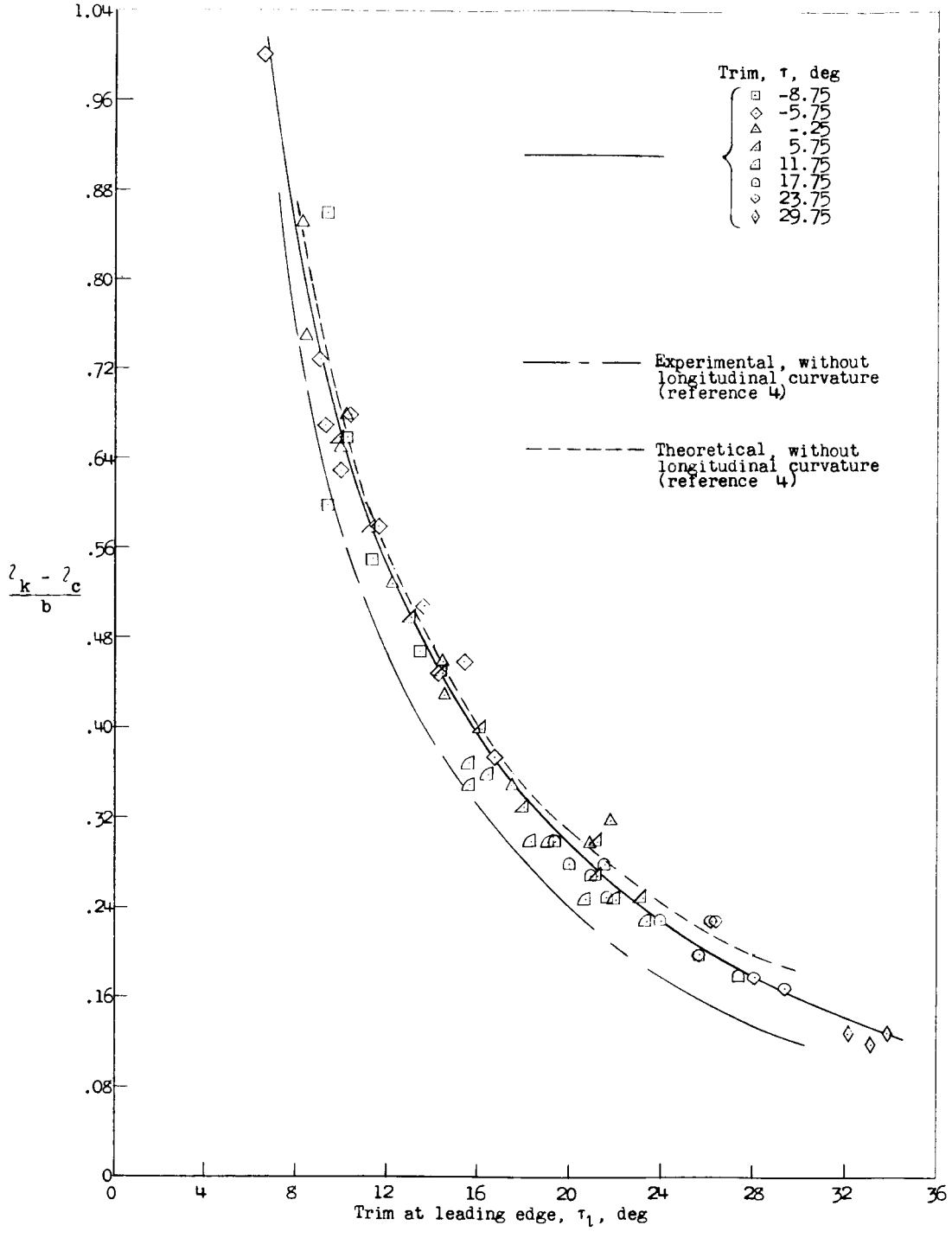

Figure 9.- Variation of $\frac{l_k - l_c}{b}$ with trim of the leading edge τ_l.

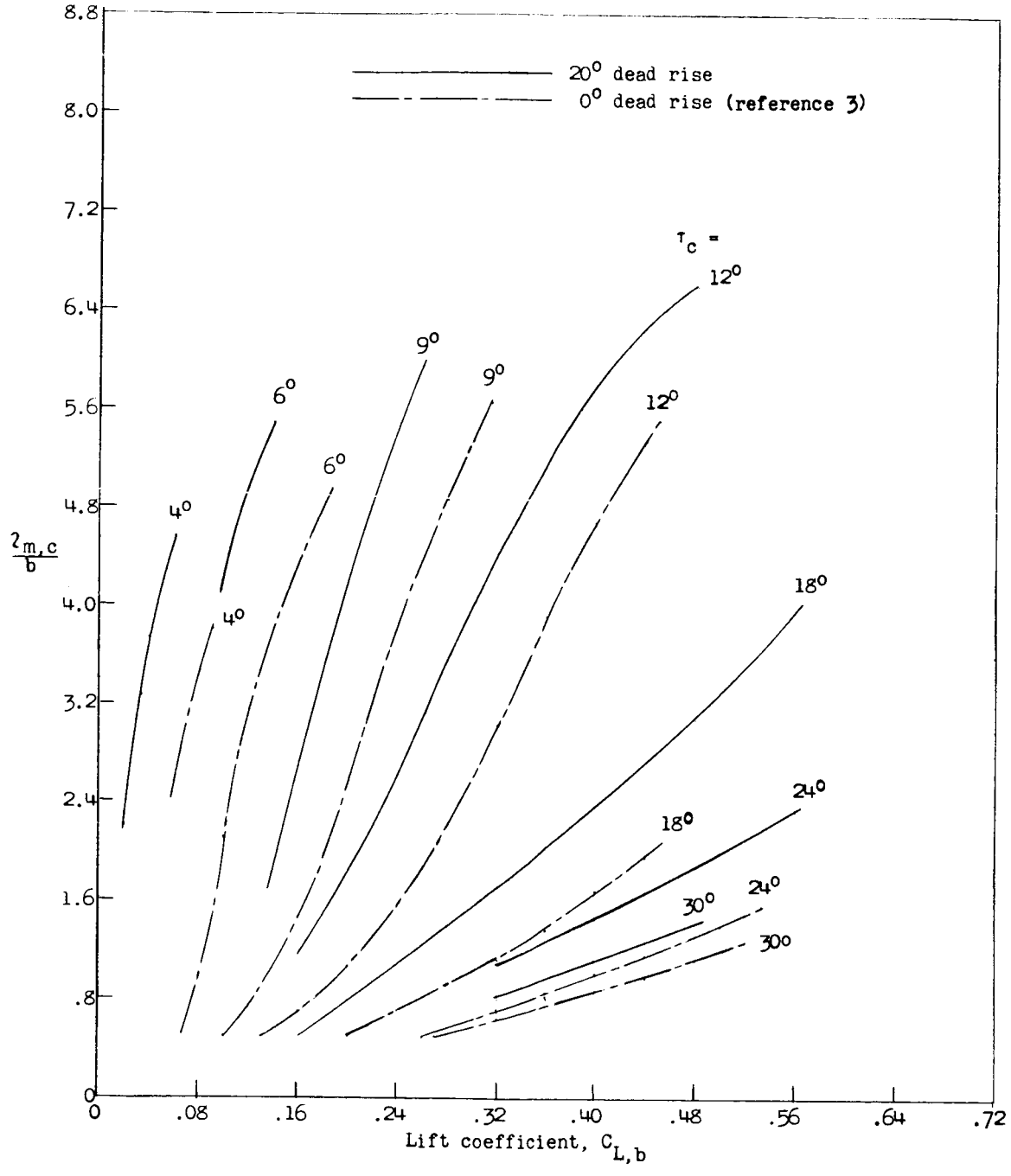

Figure 10.- Variation of the nondimensional chord of the wetted length with lift coefficient for several values of trim of the chord of the wetted length.

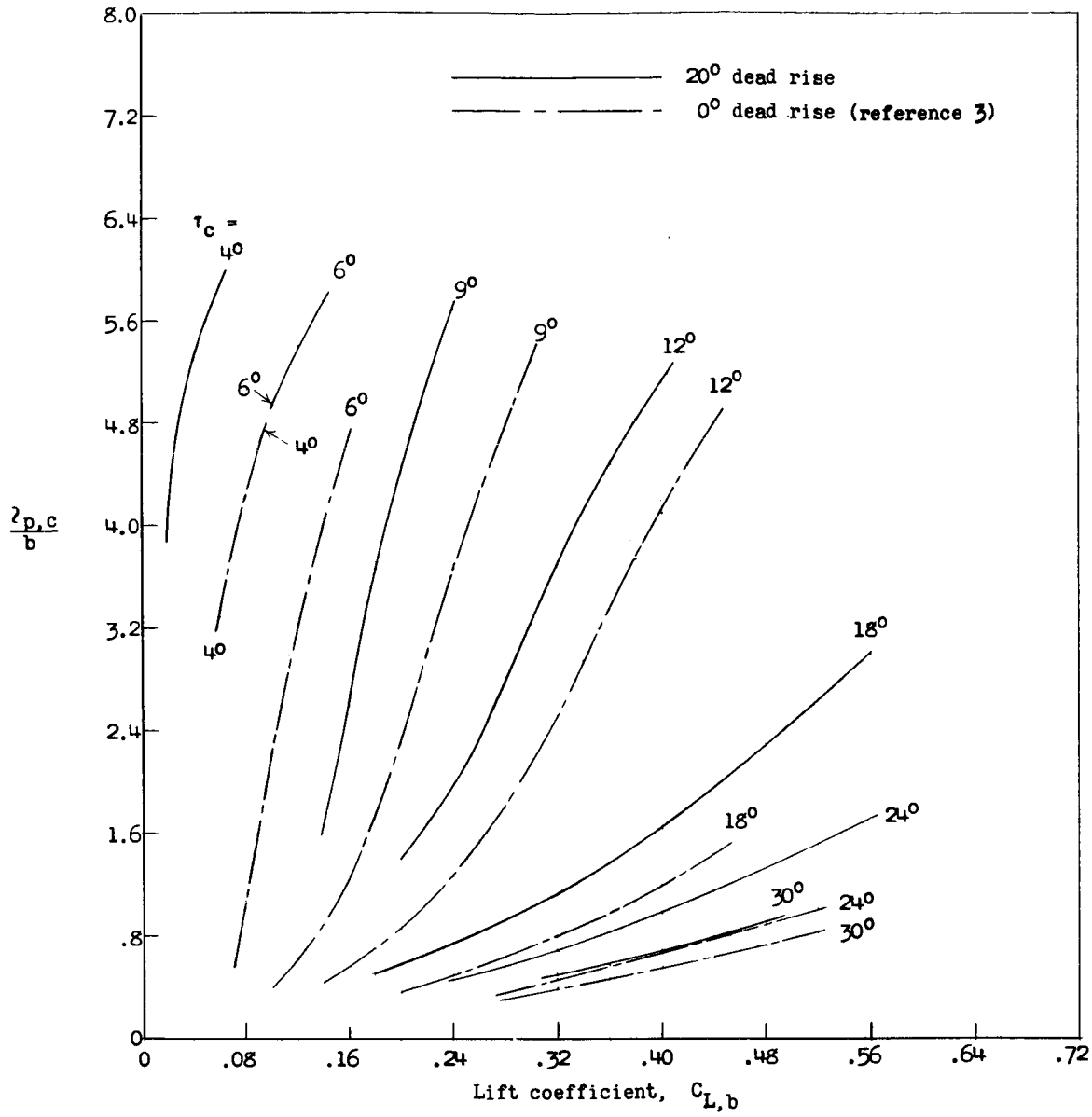

Figure 11.- Variation of nondimensional center-of-pressure location with lift coefficient for several values of trim of the chord of the wetted arc.

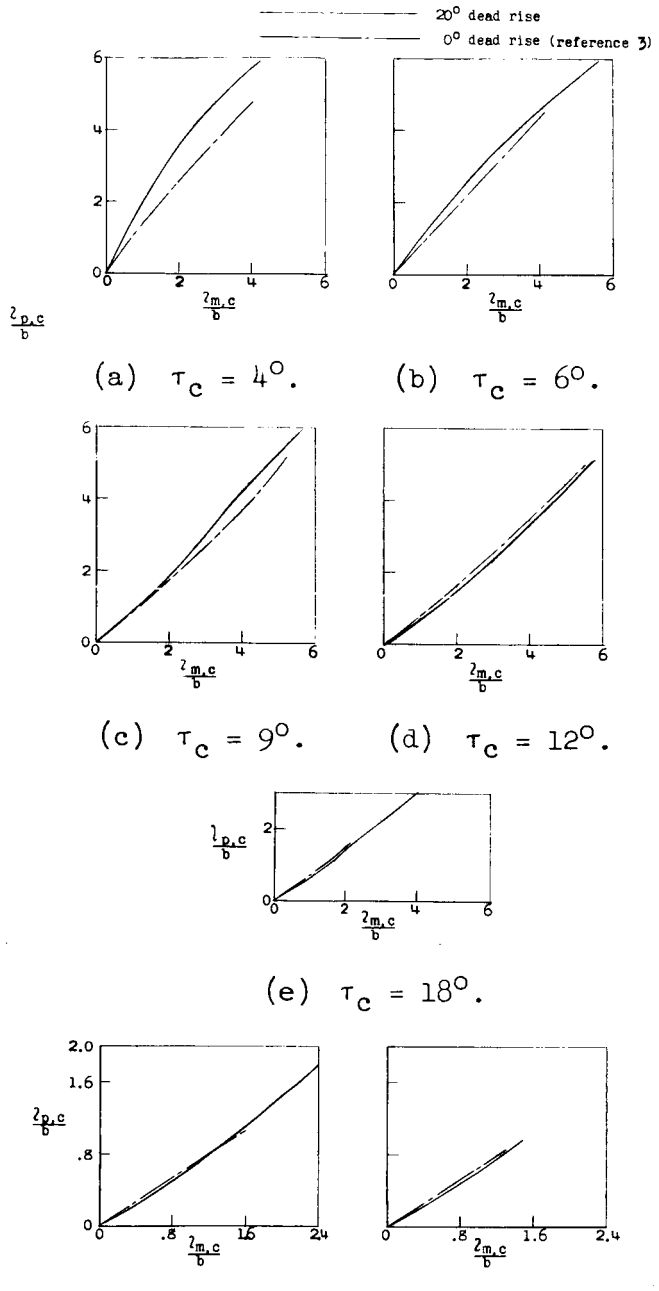

Figure 12.- Variation of nondimensional center of pressure with length-beam ratio.

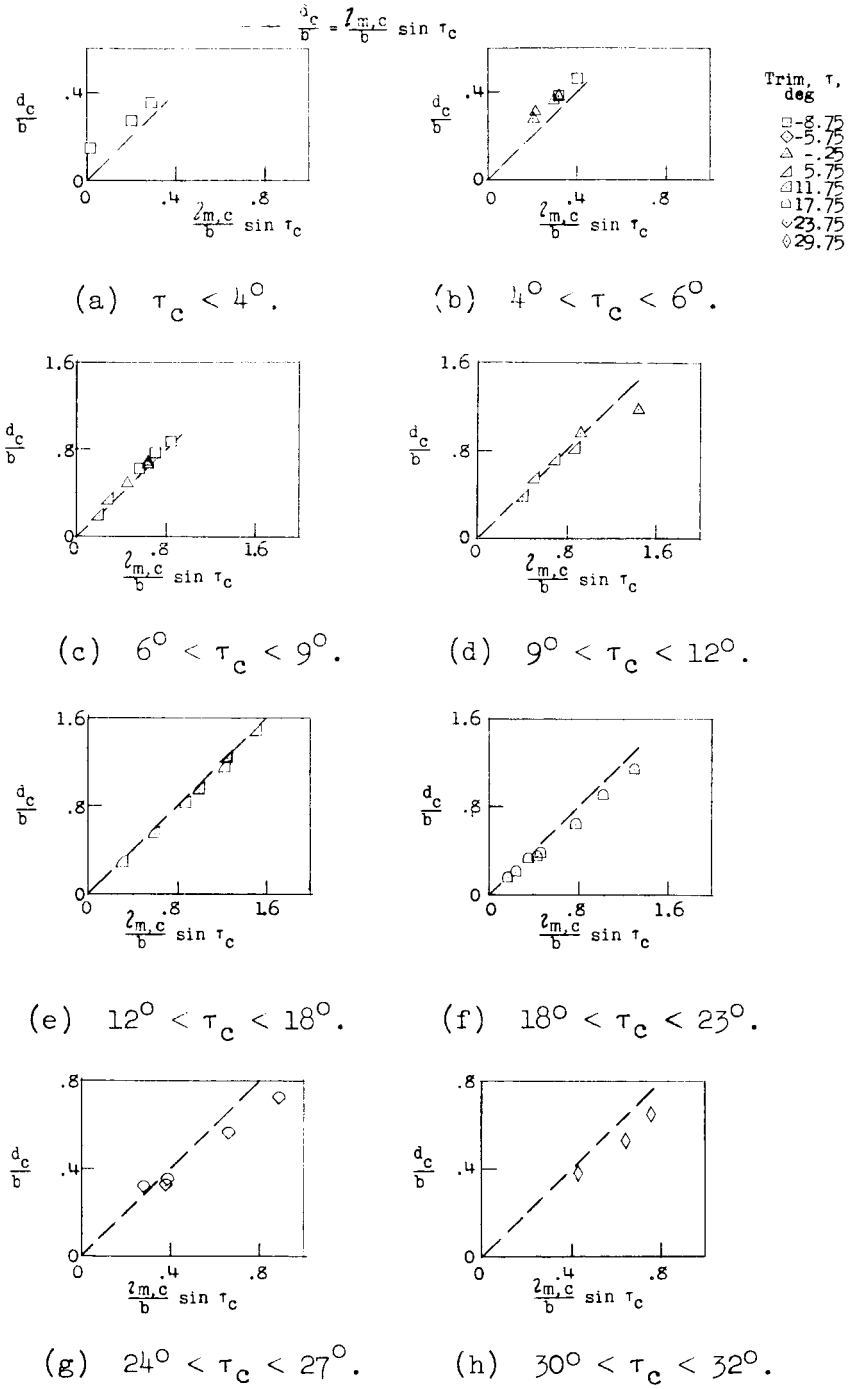

Figure 13.- Comparison of the nondimensional draft referred to the undisturbed water surface d_c/b with the nondimensional draft referred to the water surface at the leading edge $l_{m,c}/b \sin \tau_c$ for several values of trim of the chord of the wetted arc.

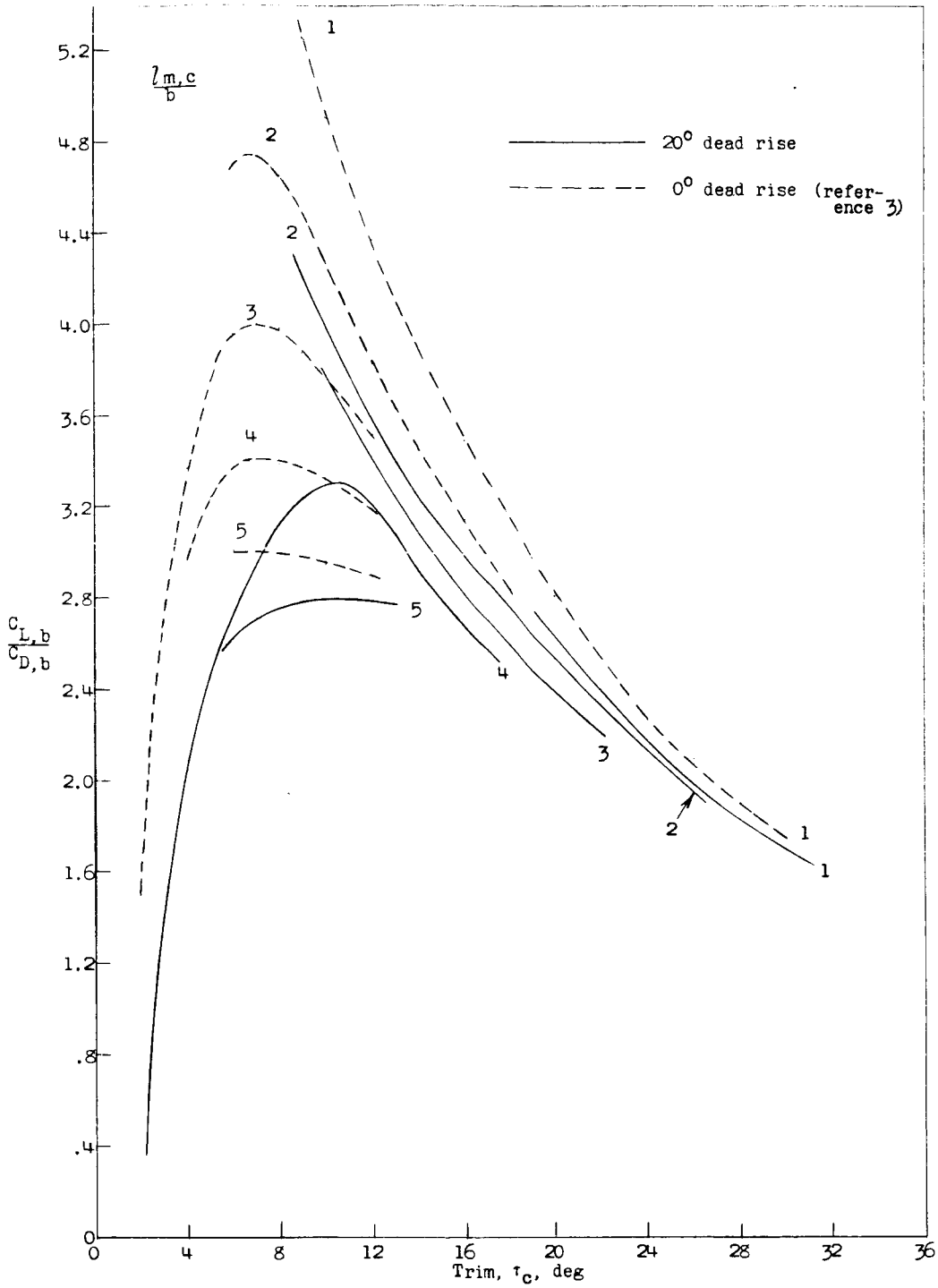

Figure 14.- Comparison of lift-drag ratios of convex surfaces with and without dead rise.

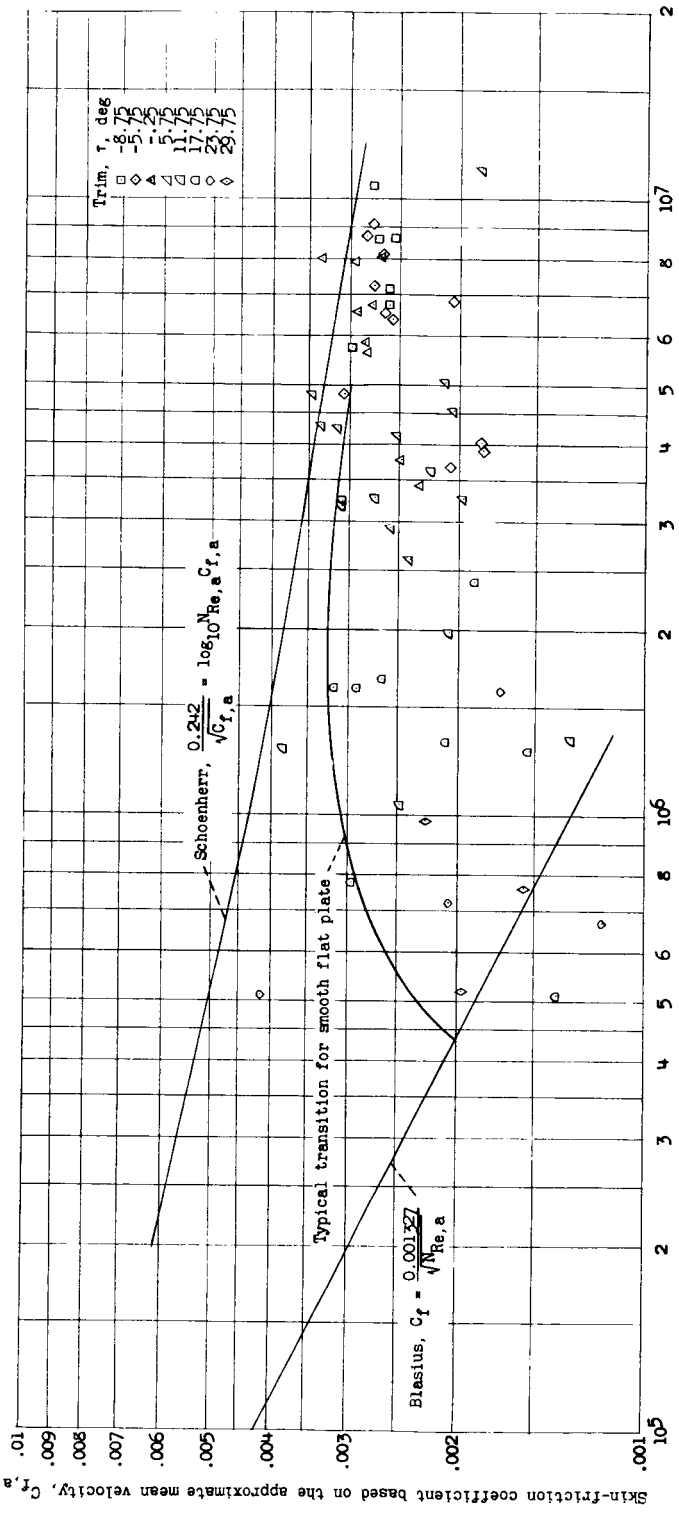

Figure 15.- Variation of skin-friction coefficient with Reynolds number. Theoretical curves obtained from reference 8.